EVS25
Shenzhen, China, Nov 5-9, 2010

Driving Torque Distribution Method for Front-and- Rear-Wheel-Independent-Drive-Type Electric Vehicles (FRID EVs) at the Time of Cornering

Nobuyoshi Mutoh[1] Osamu Nishida[1], Tatsuya Takayanagi[1],
Tadahiko Kato[2], Kazutoshi Murakami[2]

[1] *Graduate School of Tokyo Metropolitan University 6-6, Asahigaoka, Hino-shi, Tokyo, Japan*
nmutoh75@fuji.waseda.jp
[2] *Univance Corporations, 2418 Washes, Kisi-shi, Shizuoka, Japan*

Abstract

This paper describes a driving torque distribution method for front–and-rear-wheel-independent-drive-type electric vehicles (FRID EVs) in which it is possible to get stable steering on a low friction coefficient road surface. This method is characterized by distributing driving torque to the left and right wheels of the front and rear wheels, considering not only load movement of the longitudinal direction but also load movement of the lateral direction which is generated at cornering. The load movements are estimated by detecting components of the 3-axis directions, i.e., longitudinal and lateral accelerations and yaw rate, and the steering angle and friction coefficient μ *of* the road surface. The effectiveness of the proposed driving torque distribution method was verified using simulators equivalent to the prototype FRID EV simulated with Matlab/Simulink and CarSim software. This method is expected to be indispensable to improving running performance of FRID EVs.

Keywords: EV (electric vehicle), front–and-rear-wheel-independent-drive-type electric vehicles (FRID EVs), load movement, driving torque distribution, cornering, friction coefficient.

1 Introduction

Electric vehicles (EVs) are becoming important not only as an environmental measure against global warming, but also as an industrial policy [1]. In order for EVs to be used widely, the development of the next generation EVs with compatible in safety and running performance is indispensable. To meet such social requirements, the conventional propulsion force generation mechanism, i. e. motor-drive structure, which strongly influences the safety and running performance, has been investigated. Many studies on front or rear one-motor-drive-type EVs (Fig. 1(a)) have been done from the viewpoint of economical efficiency [2] and these EVs are already being marketed commercially [2]. Moreover, studies on two or four in-wheel motor-drive-type EVs (Figs. 1(b) and (c)) have also been done from the viewpoints of the control technique [3], [4], [5] and packaging [6], [7]. First, by focusing on the running performance, EVs of Figs. 1 (a) and (b) cannot cope with such dangerous vehicle problems as wheel spin and wheel lock which are caused by the load movement always generated when accelerating or decelerating [7]. When attention is paid to the safety at the time of failure, EVs of Fig. 1 (c) have difficulties with steering ability [8]. Since EVs of Fig.1(c) have more drive structures as compared with other EVs, economical efficiency and maintenance is not good, and a reliability issue may be aggravated.

Thus, after proposing front and rear wheel independent drive type electric vehicles FRID EVs (Fig. 2) compatible in safety and running performance [9], their research is being done from various angles by positioning them as a next-generation EV. It has been clarified through vehicle dynamics analysis experiments that outstanding running performance is obtained using a structural feature which can freely control longitudinal force of the front and rear wheels according to the running and road surface conditions [10]. In FRID EVs, distribution of the lateral force to the right and left tires of a front wheel and a rear wheel is performed through a differential gear like in ordinary gas-powered vehicles. Accordingly, in currently available vehicles, since sufficient lateral force required for revolution cannot be secured, under-steering (Fig. 3) is apt to be caused when cornering on a low μ-road or when cornering at high speed on a dry road. It is only the four in-wheel-motor-drive-type EV (Fig. 1 (c)) that can directly handle the longitudinal and lateral forces of four wheels [11]. However, in-wheel-motor-drive-type EVs have the serious problems cited above as a next generation EV.

Thus, a driving torque distribution method suitable for FRID EVs which can secure sufficient lateral forces of the front and rear wheels is proposed here. The lateral forces required for revolution are estimated based on the conditions regarding the friction circle in consideration of the longitudinal and lateral load movements. Here, the effectiveness of the proposed driving torque distribution method is verified using a simulator equivalent to an actual prototype FRID EV.

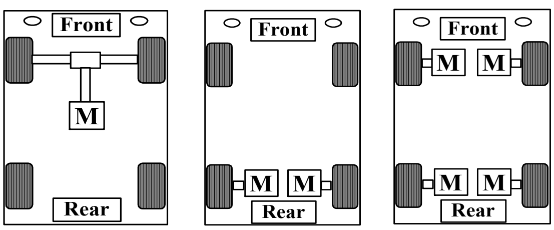

(a) Front or rear wheel drive type EV (b) Front or rear two in-wheel drive type EV (c) Four in-wheel drive type EV

Figure 1. EVs with various conventional motor drive structures.

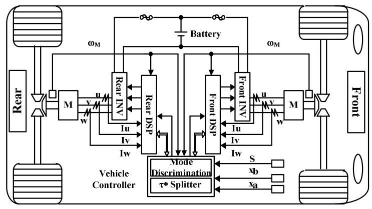

Figure 2. Front-and-rear-wheel-independent-drive-type EV (FRID EV).

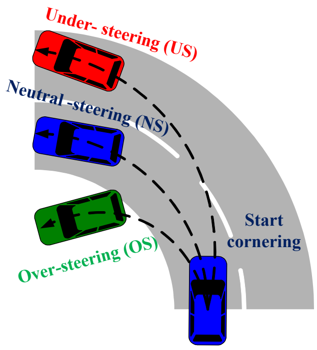

Figure 3. Situations caused by steering operations at the time of cornering.

2. Driving Torque Distribution Method at the Time of Cornering

2.1 Principal of Driving Torque Distribution at the Time of Cornering

When vehicle speed is in a steady state (which can include the standstill state), front and rear tire loads (normal forces) F_{zd_f} and F_{zd_r} act on each tire of the front and rear wheels. In this case, the vehicle is driven by the front and rear driving forces F_{xd_f} and F_{xd_r} which are supplied from front and rear motors, respectively. Shifting to an acceleration mode, the longitudinal load movement z_x to the rear wheels from the front wheels is generated. As a result, front and rear tire loads F_{zd_f} and F_{zd_r} are changed to F_{z_f} ($=F_{zd\_f} - z_x$) and F_{z_r} ($=F_{zd\_r} + z_x$) by z_x (Fig.4(b)). Therefore, in order for the vehicle to maintain ideal running based on vehicle dynamics, driving torque distribution to the front and rear wheels should be done so that the front and rear motors can generate the proper driving forces F_{x_f} and F_{x_r} corresponding to the front and rear tire loads F_{z_f} and F_{z_r} which are changed by the load movement.

Next, when starting cornering, the new lateral load movement z_y takes place between the left and right wheels. Front and rear tire loads F_{z_f} and F_{z_r} are further changed by the produced load movement z_y. For example, when cornering to the left, the left and right tire loads F_{z_fl} and F_{z_fr} , F_{z_rl}

and F_{z_fr} which act on the left and right tires of the front and rear wheels are changed to (F_{z_fl} + z_y) and (F_{z_fr} - z_y), (F_{z_rl} + z_y) and (F_{z_rr}- z_y), respectively. Here, subscripts l and r indicate left and right tires, respectively. Thus, in order for vehicles to corner stably, it is necessary to always secure the front and rear lateral forces corresponding to lateral load movement z_y. To do so, driving torque distribution should be performed according to the fact that each of the driving and braking forces and the cornering force cannot exceed the friction force μW(μ: friction coefficient, W: tire load) (Fig. 4(a)). That is, specifically, after securing lateral force required for revolution, in a friction circle, the maximum $F_{x\_j\_max}$ of the longitudinal force needed to propel the vehicle is secured by

$$F_{x\_j\_\max} = \sqrt{\mu^2 W^2 - (F_{y\_j\_\max}^2})(j = f : front, r : rear) \quad (1)$$

where $F_{y\_j\_\max} = \max(F_{y\_jl}, F_{y\_jr})(l : left, r : right)$,

$$0 \le F_{x\_j} \le F_{x\_j\_\max}.$$

Hereafter, in this study, the driving torque distribution uses the assumption that if slip angle is small, the lateral force almost agrees with the cornering force. The maximum longitudinal force $F_{x\_j\_max}$ ($j = l$: front, $j = r$: rear) obtained for each of the front and rear wheels is converted by

$$\tau_{x\_j} = k_j F_{x\_j}. \quad (2)$$

Here k_j ($j = l$ and r) is a torque conversion gain for front and rear wheels that get a match with the torque reference τ_R for the whole vehicle as generated from an accelerator which is split between the front and rear wheels by

$$\tau_R = \tau_{Rf} + \tau_{Rr}. \quad (3)$$

Here, τ_{Rf} and τ_{Rr} are the front and rear torque references split from τ_R based on the load movement. The front and rear driving torque references τ_{Rf}^* and τ_{Rr}^* are determined through comparisons between τ_{Rf} and τ_{x_f}, and between τ_{Rr} and τ_{x_r} by the next procedures:

$$\tau_{Rf}^* = \min(\tau_{Rf}, \tau_{x\_f}) \quad (4)$$

$$\tau_{Rr}^* = \min(\tau_{Rr}, \tau_{x\_r}) \quad (5)$$

where τ_{x_f} and τ_{x_r} are the front and rear driving references determined from the front and rear lateral forces F_{y_f} and F_{y_r}.

Finally, in order to secure the stability of the front and rear wheels the above driving torque references τ_{Rf}^* and τ_{Rr}^* are compensated for according to the following slip ratio conditions (Fig. 5).

if $s_{f\_l}, or, s_{f\_r} > 0.2,$ then $\tau_{Rf}^* = 0,$

where $s_{f\_l} = (r_{eff}\omega_{f\_l} - V) / r_{eff}\omega_{f\_l};$

$$s_{f\_r} = (r_{eff}\omega_{f\_r} - V) / r_{eff}\omega_{f\_r}. \quad (6)$$

if $s_{r\_l}, or, s_{r\_r} > 0.2,$ then $\tau_{Rr}^* = 0,$

where $s_{r\_l} = (r_{eff}\omega_{r\_l} - V) / r_{eff}\omega_{r\_l};$

$$s_{r\_r} = (r_{eff}\omega_{r\_r} - V) / r_{eff}\omega_{r\_r}. \quad (7)$$

Here r_{eff} is effective radius of a tire; V is vehicle speed; ω_{f_l} and ω_{f_r} are angular speeds of the left and right tires of the front wheels; and ω_{r_l} and ω_{r_r} are angular speeds of the left and right tires of the rear wheels. Under the slip ratio conditions of other than (6) and (7), the torque references τ_{Rf}^* and τ_{Rr}^* to satisfy the procedures of (4) and (5) become the actual torque references for the front and rear torque controllers.

As shown in the flow chart of Fig. 6, according to the steering angle δ, the driving torque references are distributed to the front and rear wheels, dividing the two driving torque distribution procedures into a procedure to determine the distribution from longitudinal forces based on the torque reference generated from accelerator. Hereafter, each procedure is described in detail.

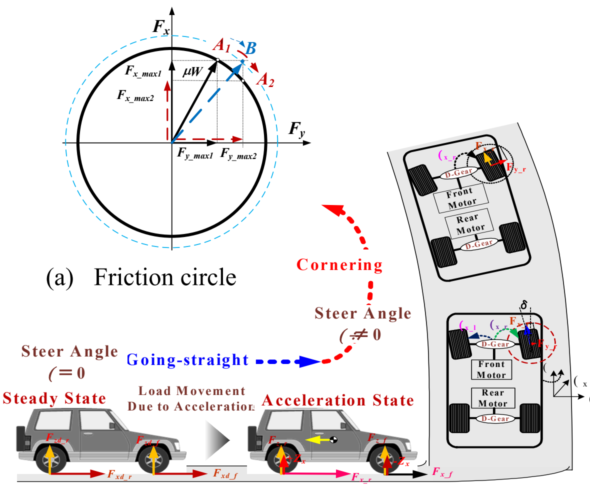

(a) Friction circle

(b) Difference of the torque distribution when going straight and cornering

Figure 4. Basic points which should be taken into consideration when distributing driving torque.

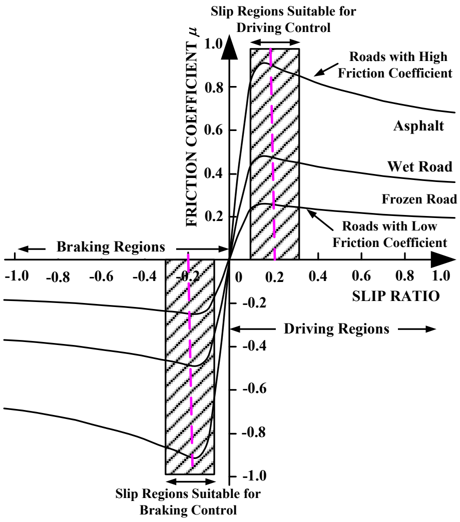

Figure 5. Stability operation domain of slip ratio.

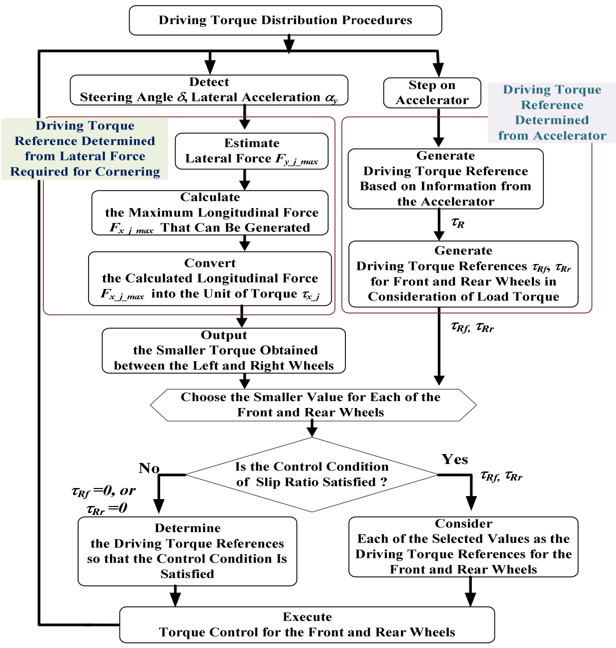

Figure 6. Flow chart explaining the basic principal of the driving torque distribution method.

2.2 A Procedure to Determine Driving Torque Distributed to the Front and Rear Wheels Based on Torque Reference Obtained from the Accelerator

The main point of this procedure is to distribute longitudinal forces to the front and rear wheels in consideration of load movement caused by acceleration and deceleration. Then, first, longitudinal load movement z_x is derived using a moment diagram of forces acting on a vehicle which is in a standstill state (Fig. 7(a)) and an accelerating state (Fig. 7(b)). In a standstill state, the vehicle load which acts on the center of gravity is distributed to the normal forces F_{zd_f} and F_{zd_r} on the front and rear tires by

$$F_{Zd\_f} = \frac{L_r}{L_{car}} \cdot F_{mg}, F_{Zd\_r} = \frac{L_f}{L_{car}} \cdot F_{mg}. \tag{8}$$

When vehicles are accelerated, the force moments acting on the contacting points (X and Y) of the front-and-rear wheels are given by

$$-L_{car} \cdot F_{z\_f} + L_r \cdot F_{mg} - \frac{F_{mg}}{g} \cdot \alpha_{car} \cdot H_{car} = 0 \tag{9}$$

and

$$-L_f \cdot F_{mg} + L_{car} \cdot F_{z\_r} - \frac{F_{mg}}{g} \cdot \alpha_{car} \cdot H_{car} = 0 \tag{10}$$

where vehicle weight $F_{mg} = mg$ (m: vehicle mass, g: acceleration due to gravity); α_{car}: longitudinal acceleration; H_{car}: height of the center of gravity; L_{car}: wheelbase of a vehicle; and L_f: length between the axles of the front wheels and the center of gravity. Therefore, the normal forces (F_{z_f} and F_{z_r}) which act on the tire of the front and rear wheels are expressed by

$$F_{z\_f} = F_{Zd\_f} - \frac{H_{car}}{L_{car}} \cdot \frac{\alpha_{car}}{g} \cdot F_{mg} = F_{Zd\_f} - z_x \tag{11}$$

and

$$F_{z\_r} = F_{zd\_r} + \frac{H_{car}}{L_{car}} \cdot \frac{\alpha_{car}}{g} \cdot F_{mg} = F_{zd\_r} + z_x \tag{12}$$

where $z_x = \frac{H_{car}}{L_{car}} \cdot \frac{\alpha_{car}}{g} \cdot F_{mg} = \frac{H_{car}}{L_{car}} \cdot F_{car} (F_{car} = M_{car}\alpha_{car})$.

Using F_{z_f}, F_{z_r} and friction coefficient μ of a road surface, the longitudinal forces (F_{x_f} and F_{x_r}) acting between road surfaces and the tires of the front and rear wheels are given by

$$F_{x\_f} = \mu(F_{zd\_f} - z_x) = \mu(F_{zd\_f} - \frac{F_{car} \cdot H_{car}}{L_{car}}) \tag{13}$$

and

$$F_{x\_r} = \mu(F_{zd\_r} + z_x) = \mu(F_{zd\_r} + \frac{F_{car} \cdot H_{car}}{L_{car}}). \tag{14}$$

Then, so that the front and rear motors can generate the driving torques corresponding to these longitudinal forces, torque references τ_{Rf} and τ_{Rr} are distributed to the front and rear torque controllers by

$$\tau_{Rf} = k_f \cdot R_f \cdot \tau_R \tag{15}$$

and

$$\tau_{Rr} = k_r \cdot R_r \cdot \tau_R (R_r = 1 - R_f). \tag{16}$$

Here the front distribution ratio R_f is given by

$$R_f = \frac{F_{x\_f}}{F_{x\_f} + F_{x\_r}} = \frac{\mu(F_{zd\_f} - z_x)}{\mu \cdot M_{car}} = \frac{M_f \cdot g - z_x}{M_{car} \cdot g}. \tag{17}$$

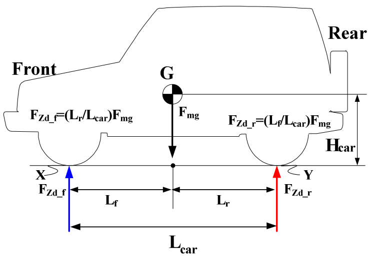

(a) Standstill

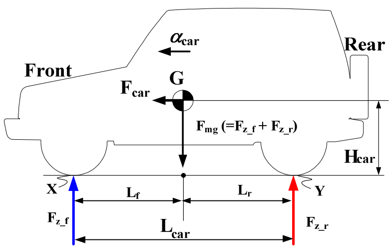

(b)Accelerating state.

Figure 7. Moment diagram of forces acting on a vehicle.

2.3 A Procedure to Determine Driving Torque Distribution Based on Lateral Force Required for Cornering

Here, using Fig. 8, movement of vehicles is described, by transposing to a two-wheel model equivalent to the four-wheel model of vehicles in general. Assuming that the steering angle δ and the slip angle β of vehicle are small, the lateral motion of the vehicle and the yaw dynamics at the center of gravity of the vehicle are studied that can be handled using longitudinal and lateral accelerations α_x and α_y, and yaw rate γ detected from the 3-axis acceleration sensor installed at the center of gravity of the vehicle. The lateral motion for front and rear wheels is expressed by

$$M_{car}\alpha_y = 2F_{y\_f}\cos\delta + 2F_{y\_r}. \tag{18}$$

Taking the moment balance about the z-axis into consideration, the equation for yaw dynamics is given by

$$I_z \cdot \dot{\gamma} = 2F_{y\_f} L_f \cos\delta - 2F_{y\_r} L_r \tag{19}$$

where I_z is yaw moment of inertia about the z-axis. Solving (18) and (19) about F_{y_f} and F_{y_r}, the front and rear lateral forces are derived as

$$F_{y\_f} = \frac{I_z \cdot \dot{\gamma} + M_{car}\alpha_y L_r}{2(L_f + L_r)\cos\delta} \tag{20}$$

and

$$F_{y\_r} = \frac{-I_z \cdot \dot{\gamma} + M_{car}\alpha_y L_f}{2(L_f + L_r)} \tag{21}$$

Next, the lateral load movement z_y appearing during cornering is obtained by considering roll moment at the center of gravity of the vehicle shown in Fig. 9. Moment balance at the center of gravity of the vehicle yields the equation for the normal force F_{z_l} on the left tires of the front and rear wheels as

$$F_{z\_l} = \frac{M_{car}\, g}{2} + \frac{F_{car}\, H_{car}}{b}. \tag{22}$$

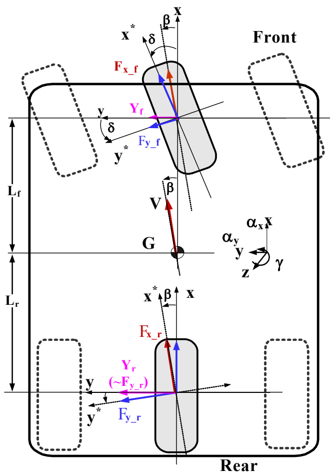

Figure 8. Two-wheel vehicle model equivalent to a four-wheel vehicle (left turn).

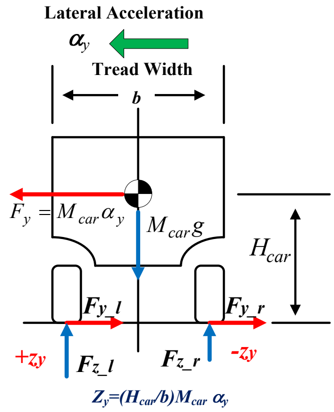

Figure 9. Roll moment which acts at the time of a left turn.

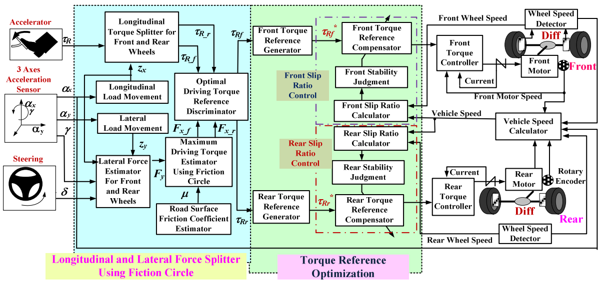

Figure 10. Control block diagram of the torque controller when the proposed driving torque distribution method is applied to the FRID EV.

Accordingly, using the obtained F_{z_l} and (9), the lateral load movement z_y is obtained by

$$z_y = F_{z\_l} - W_l = \frac{M_{car}\alpha_y \cdot H_{car}}{b} (W_l = M_{car} g / 2). \tag{23}$$

By using the derived z_y, the left-and-right-normal forces F_{z_fl} and F_{z_fr} on tires for the front wheels, and the left-and-right-normal forces F_{z_rl} and F_{z_rr} on tires for the rear wheels are given as follows:

$$F_{z\_fl} = (F_{zd\_f} - z_x) + z_y = \frac{M_{car}(L_r g - H_{car}\alpha_x)}{L_{car}} + \frac{H_{car}}{b} M_{car}\alpha_y, \tag{24}$$

$$F_{z\_fr} = \frac{M_{car}(L_r g - H_{car}\alpha_x)}{L_{car}} - \frac{H_{car}}{b} M_{car}\alpha_y, \tag{25}$$

$$F_{z\_rl} = (F_{zd\_r} + z_x) - z_y = \frac{M_{car}(L_f g + H_{car}\alpha_x)}{L_{car}} + \frac{H_{car}}{b} M_{car}\alpha_y, \tag{26}$$

and

$$F_{z\_rr} = \frac{M_{car}(L_f g + H_{car}\alpha_x)}{L_{car}} - \frac{H_{car}}{b} M_{car}\alpha_y. \tag{27}$$

Considering that the front and rear lateral forces $2F_{y\_f}$ and $2F_{y\_r}$ of (20) and (21) are divided with ratios of $F_{z\_fl} : F_{z\_fr}$, and $F_{z\_rl} : F_{z\_rr}$, respectively, the left and right lateral forces F_{y_fl} and F_{y_fr} of the front wheels and the left and right lateral forces F_{y_rl} and F_{y_rr} of the rear wheels are expressed by

$$F_{y\_fl} = 2F_{y\_f} \frac{F_{z\_fl}}{F_{z\_fl} + F_{z\_fr}}, \tag{28}$$

$$F_{y\_fr} = 2F_{y\_f} \frac{F_{z\_fr}}{F_{z\_fl} + F_{z\_fr}}, \tag{29}$$

$$F_{y\_rr} = 2F_{y\_r} \frac{F_{z\_rr}}{F_{z\_rl} + F_{z\_rr}}, \tag{30}$$

and

$$F_{y\_rl} = 2F_{y\_r} \frac{F_{z\_rl}}{F_{z\_rl} + F_{z\_rr}}. \tag{31}$$

3. Verification of the Proposed Driving Torque Distribution Method by Simulations

Simulations are performed using a prototype FRID EV with the following specifications. m: 1900 kg; H_{car}: 670 mm; L_f:1500 mm, L_r:1125 mm; L_{car}: 2625 mm. Fig. 12 shows simulation results when turning toward the left on a low μ-road (μ = 0. 2) with a 3-deg steering angle at 3 s after accelerating. First, the proposed driving torque distribution method is evaluated through simulations under the severe driving condition of turning to the left on the low μ- road. When the proposed method is not applied (Fig. 12(a)), at around 2 s after stating cornering the slip angle of

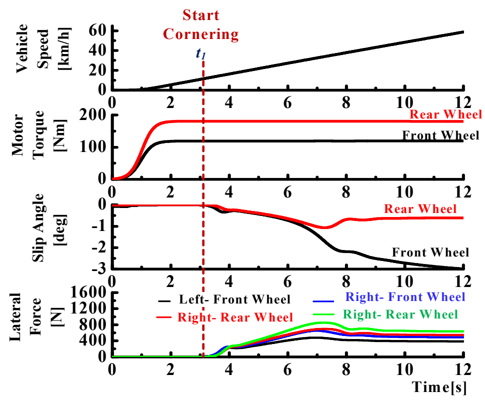

(a)When lateral force is not distributed to the front and rear wheels properly.

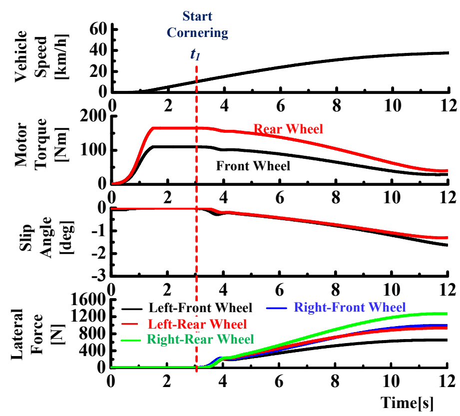

(b)When lateral force is distributed to the front and rear wheels properly.

Figure 12. Effects of the proposed driving torque distribution method on a very low μ-road when cornering on a low μ-load (μ = 0.2) at steering angle 3 deg.

the front wheels is increasing gradually and the front and rear lateral forces are saturated. As a result, the vehicle shifts from the travelling lane, without the ability to corner (Fig.13). On the other hand, when the proposed method is applied, the saturation of lateral forces is suppressed by making driving forces of the front and rear wheels decrease with cornering. Since the lateral forces required for cornering are secured (Fig. 12(b)), the vehicle can turn to the left along the travelling lane (Fig.13).

Next, the proposed method is evaluated under severer conditions that make the vehicle accelerate while cornering on an ultra low μ-road (μ = 0. 1). The difference in the cornering performance between the proposed method and the conventional slip control is also made clear. Fig. 14 shows the simulation results under the conditions that the vehicle turns to the left at a 3-deg steering angle while accelerating on the ultra low μ-road at time t_1 at about 10 s after stating. When the proposed method is not applied (Fig. 14(a)), the slip ratio immediately increases to 1. Then, the wheel spin occurs, and a skid is caused. Since sufficient lateral forces required for revolution cannot be secured, the vehicle

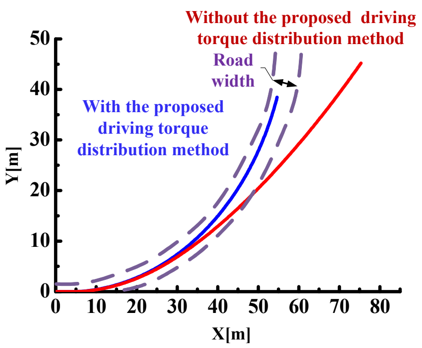

(a)Vehicle trajectories

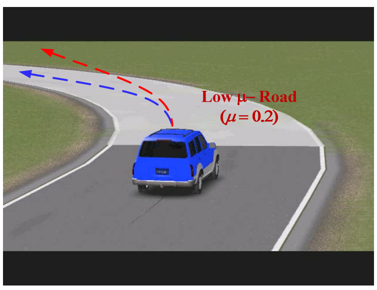

(b)Road condition used for simulations

Figure 13. Effects of the proposed driving torque distribution method on vehicle trajectories under the same simulation conditions as Fig.12.

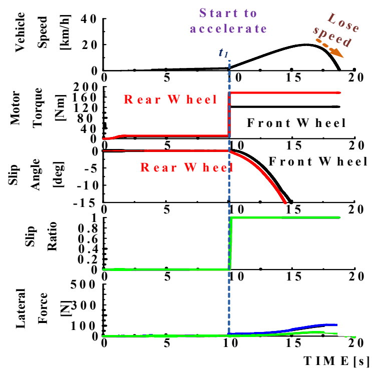

(a)Without proposed torque distribution method.

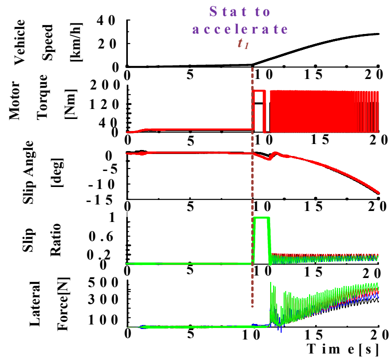

(b) With proposed torque distribution method

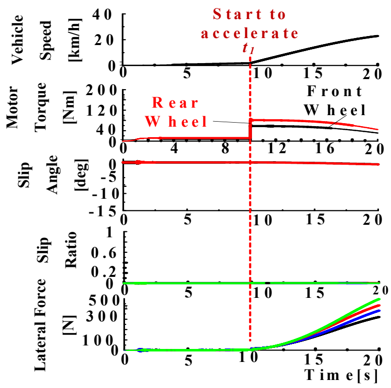

(c) With proposed torque distribution method

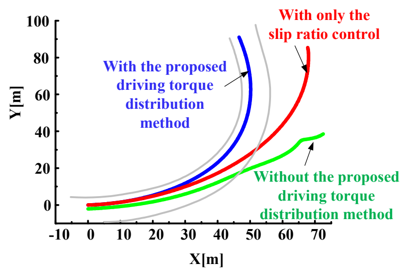

(d) Vehicle trajectories when cornering while accelerating

Figure 14. Effects of the proposed driving torque distribution method when starting at a corner on an ultra low μ-road while accelerating (μ = 0.1, steering angle =3 deg).

strays from the travelling lane without being able to corner (Fig. 14(d)). Moving to the case of the slip ratio control, when making a vehicle accelerate, slip ratios are soon increased to 1, and although once they lead to the wheel spin state, they are suppressed to less than 0. 2 and then the

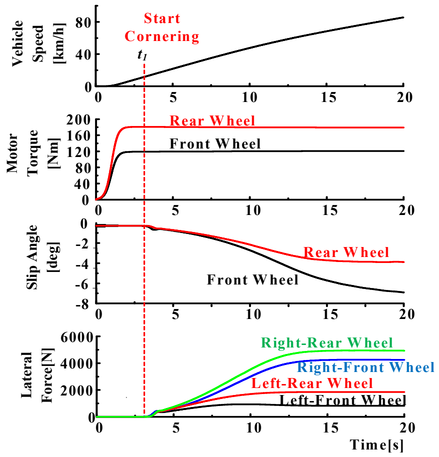

(a)Without the proposed torque distribution method

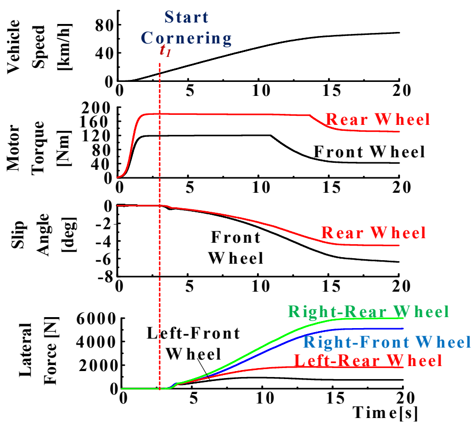

(b)With the proposed torque distribution method

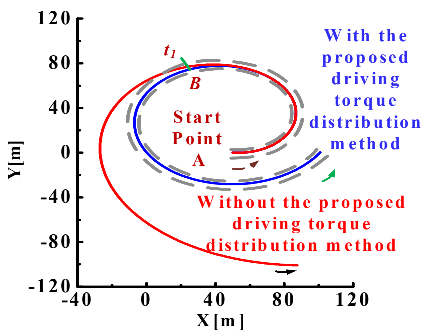

(c)Vehicle trajectories

Figure 15. Effects of the proposed driving torque distribution method when cornering on a high μ-road while accelerating (steering angle= 3 deg, μ =0.75).

wheel spin state is avoided. However, the slip angle increased gradually (Fig. 14(a)), and eventually, the vehicle cannot turn to the left (Fig. 14 (d)). On the other hand, when the proper driving torque is applied to front and rear wheels using the proposed driving torque distribution method, the slip ratio is kept at a value near zero and skidding is also not seen. Then, lateral forces required for revolution are also secured, and the vehicle can turn to the left properly along the traveling lane (Figs. 14 (c) and (d)).

Finally, the effects when turning to the left at high speeds on the high μ-road (μ = 0. 75) are investigated under the conditions of beginning to turn to the left at the time t_1 while accelerating. When the proposed driving torque distribution method is not applied, the vehicle can turn to the left properly up to corner B along the traveling lane, 10 s after starting to accelerate (Figs. 15(a) and (c)).However, it is impossible to secure the lateral forces required for revolution because they are gradually saturated after passing B point. As a result, the vehicle cannot run along the road, and it is accelerating too much.

On the other hand, when the proposed driving torque distribution method is applied, lateral forces required for revolution are secured by decreasing the front and rear motor torques in accordance with increase in speeds, and the turn to the left can be effectively carried out to bring the vehicle to the final destination.

4. Conclusion

When cornering on low μ-roads or at high speeds, it is very difficult for all conventional vehicles to perform steering for revolution. This paper described a driving torque distribution method to solve these problems using the FRID EV structural feature that it can freely distribute driving forces to the front and rear wheels according to road surface and running conditions. The driving torque distribution method is characterized by distributing the front and rear torques to the front and rear motors so that lateral forces required for revolution can be secured based on the information about steering angle, friction coefficient, and the lateral and longitudinal accelerations. The effectiveness of the proposed driving torque distribution method was verified through simulations about the cornering performance on low μ-roads and at high speeds.

Furthermore, in addition to the method of controlling the FRID EVs which was previously developed, the method proposed here has added a still more powerful function to FRID EVs from the viewpoints of safety and running performance.

References

[1] K. T. Chua, C. C. Chan, and C. Liu, "Overview of permanent-magnet brushless drives for electric and hybrid electric vehicles," *IEEE Trans. Ind. Electron.*, vol. 55, no. 6, pp. 2246–2257, 2008.

[2] Mitsubishi innovative Electric Vehicle, "imides", http://www.mitsubishi-motors.co.jp/corporate/technology/environment/miev.html.

[3] Y. E. Zhao, J. W. Zhang, and X. Q. Guan, "Modeling and simulation of electronic differential system for an electric vehicle with two-motor-wheel drive," IEEE *Intelligent Vehicles Symposium 2009*, 3–5 June 2009, Xi'an, China, pp. 1209–1214.

[4] F. Tahami, R. Kazemi, and S. Farhanhi, "A novel driver assist system for all-wheel-drive electric vehicles," *IEEE Trans. on VT*, vol. 52, no. 2, pp. 683–692, 2003.

[5] M. Terashima, T. Ashikaga, T. Mizuno, K. Natori, N. Fujiwara, and M. Yada, "Novel motors and controllers for high performance electric vehicle with four in-wheel motors," *IEEE Trans. Ind. Electron.*, vol. 44, no. 1, pp. 28–38, 1997.

[6] H. Shimizu, J. Harada, C. Bland, K. Kawakami, and L. Chan, "Advanced Concepts in Electric Vehicle Design," *IEEE Trans. Ind. Electron.*, vol. 44, no. 1, pp. 14–18, 1997.

[7] N. Mutoh, Y. Hayano, H. Yahagi, and K. Takita, "Electric Braking Control Methods for Electric Vehicles With Independently Driven Front and Rear Wheels," IEEE Trans. on IES, Vol. 54, No. 2, 2007.

[8] N. Mutoh, Y. Takahashi, and Y. Tomita, "Failsafe drive performance of FRID electric vehicles with the structure driven by the front and rear wheels independently," *IEEE Trans. Ind. Electron.*, vol. 55, no. 6, pp. 2306–2315, 2008.

[9] N. Mutoh, Y. Miyazaki, R. Masaki, F. Tajima, and T. Ohmae, "Electric drive system and drive method", U.S Patent 5549172.

[10] N. Mutoh and Y. Takahashi, "Front-and-rear-wheel-independent-drive type electric vehicle (FRID EV) with the outstanding driving performance suitable for next-generation advanced EVs", IEEE VPPC2009, Dearborn, MI, 7-10 Sept. 2009, pp. 1064 – 1070.

[11] X. Lu and Y. Zhupping, "Control allocation of vehicle dynamics control for a 4 in-wheel-motored EV", PEITS, Shenzhen, 19-20 Dec. 2009, pp. 307 – 311.

Authors

Dr. Nobuyoshi Mutoh, Professor, Graduate School of Tokyo Metropolitan University, Major fields are advanced echo-machine control systems such as EVs. PV, wind power and fuel cells. IEEE senior member, Professional Engineer (Electronics and Electronics)

Mr. Osamu Nishida
Honda Motors Co. Ltd. He received the BS degree in the Department of Systems, Tokyo Metropolitan University. His area of research is EV control system.

Mr, Tatsuya Takayanagi
He is currently working towards the M.S degree in the Development of Systems Design of Graduate School, Tokyo Metropolitan University, Tokyo, Japan.

Mr. Tadahiko Kato
Fellow, General Manager, Advanced Product Development Department, Univance Co.

Mr. Kazutoshi Murakami
Manager, DT Promotion Section, Advanced Product Development Department, Univance Co.